

# ULRR

## Investigation of the magnetization reversal mechanism of electrolessly deposited Co-B nanotubes

Item Type	Article
Authors	Richardson, David;Kingston, Samuel;Rhen, Fernando
Citation	AIP Advances;6, 056113
Publisher	American Institute of Physics
Download date	2026-06-13 09:08:02
Item License	<a href="https://creativecommons.org/licenses/by-nc-sa/1.0/">https://creativecommons.org/licenses/by-nc-sa/1.0/</a>
Link to Item	<a href="https://hdl.handle.net/10344/4982">https://hdl.handle.net/10344/4982</a>



## Investigation of the magnetization reversal mechanism of electrolessly deposited Co-B nanotubes

David Richardson, Samuel Kingston, and Fernando M. F. Rhen

Citation: *AIP Advances* **6**, 056113 (2016); doi: 10.1063/1.4943603

View online: <http://dx.doi.org/10.1063/1.4943603>

View Table of Contents: <http://scitation.aip.org/content/aip/journal/adva/6/5?ver=pdfcov>

Published by the *AIP Publishing*

---

### Articles you may be interested in

[Magnetic interactions and reversal mechanisms in Co nanowire and nanotube arrays](#)

*J. Appl. Phys.* **113**, 093907 (2013); 10.1063/1.4794335

[Magnetization configurations and reversal of thin magnetic nanotubes with uniaxial anisotropy](#)

*J. Appl. Phys.* **108**, 083920 (2010); 10.1063/1.3488630

[Reversal modes in magnetic nanotubes](#)

*Appl. Phys. Lett.* **90**, 102501 (2007); 10.1063/1.2437655

[Electroless polyol deposition and magnetic properties of nanostructured Ni 50 Co 50 films](#)

*J. Appl. Phys.* **88**, 2125 (2000); 10.1063/1.1305826

[Magnetization reversal mechanism of Co–O films with oblique anisotropy](#)

*J. Appl. Phys.* **85**, 4714 (1999); 10.1063/1.370457

---

A promotional banner for AIP Applied Physics Reviews. It features a blue and orange background with a molecular structure graphic. On the left is a thumbnail of a journal cover. The main text reads 'NEW Special Topic Sections' in large white letters. Below this, it says 'NOW ONLINE' in orange, followed by 'Lithium Niobate Properties and Applications: Reviews of Emerging Trends' in white. The AIP Applied Physics Reviews logo is in the bottom right corner.

**NEW Special Topic Sections**

**NOW ONLINE**  
Lithium Niobate Properties and Applications:  
Reviews of Emerging Trends

**AIP** Applied Physics Reviews

## Investigation of the magnetization reversal mechanism of electrolessly deposited Co-B nanotubes

David Richardson, Samuel Kingston, and Fernando M. F. Rhen  
*Department of Physics and Energy, Materials and Surface Science Institute, University of Limerick, Ireland*

(Presented 14 January 2016; received 3 November 2015; accepted 22 December 2015; published online 4 March 2016)

Co-B nanotubes were prepared via an electroless deposition method. The morphology, magnetic properties and the magnetization reversal mechanism of the nanotubes were investigated. Deposition was carried out in porous polycarbonate membranes leading to the formation of Co-B nanotubes with an average external diameter of 400 nm and lengths up to 6  $\mu\text{m}$ . Electroless deposition resulted in the formation of alloys with composition  $\text{Co}_{70}\text{B}_{30}$  and a specific magnetization of  $65.6 \text{ J T}^{-1}\text{kg}^{-1}$ , which is about 40 % of that of pure Co ( $161 \text{ J T}^{-1}\text{kg}^{-1}$ ). The transversal and vortex modes were identified as the mechanisms responsible for magnetization reversal in the nanotubes. A crossover between the two modes is observed at low angles and the results are in line with current models for switching mechanisms of nanotubes. © 2016 Author(s). All article content, except where otherwise noted, is licensed under a Creative Commons Attribution 3.0 Unported License. [<http://dx.doi.org/10.1063/1.4943603>]

### I. INTRODUCTION

There is a growing research interest on the synthesis of nanotubes and the investigation of their magnetic properties following a similar trend observed for nanowires.<sup>1</sup> Many of the merits associated with nanotubes as active magnetic materials stem from the behaviour of the magnetic domains within the tube walls.<sup>2</sup> Theoretically, the advantages that the tubular geometry has over the wire geometry are due to the fact that it avoids singularity in micro-magnetic distribution.<sup>3</sup> The core-free magnetic configuration leads to uniform switching fields and guaranteed reproducibility.<sup>4</sup> In addition, while nanowires offer only two geometric parameters, the wall thickness of tubular nanostructures gives an extra degree of freedom. The understanding of magnetization reversal mechanisms is closely related to the coercivity of magnetic nanostructures.<sup>5</sup> Generally, the magnetization reversal mechanism depends on the ratio between the inner and the outer diameters of the nanotubes. Han *et al.* have reported for a series of nanotubes that the reversal mechanism can occur by the nucleation and movement of the domain walls or by coherent rotation of the magnetic moments.<sup>4</sup>

Many of the reported synthesis techniques for nanowires and nanotubes rely on template-based synthesis using electrochemical or electroless deposition.<sup>6–9</sup> Electroless deposition has acquired much interest as it is one of the simplest and cheapest methods of nanostructure preparation in terms of required equipment and processing steps. In addition, the search for novel tuneable physical, chemical and magnetic properties has motivated an extensive investigation of a diverse range of electrolessly-deposited alloys.<sup>10–12</sup>

In this manuscript, we have prepared Co-B nanotubes by electroless deposition and investigated the magnetization reversal mechanism. Despite the fact that the morphology of the electrolessly deposited Co-B nanotubes is similar to that of Ni-B and Ni-Fe-B, which we have previously investigated, the magnetization reversal mechanism is quite different.

### II. EXPERIMENTAL PROCEDURES

The templates used for the electroless deposition of the Co-B nanotubes were Whatman cyclopore track-etched polycarbonate membranes. The average pore lengths and pore diameters are



20  $\mu\text{m}$  and 400 nm, respectively. Activation of the membranes was carried out prior to deposition via a two-step process. First, the membranes were immersed in a sensitization solution of 0.24 M HCl and 0.013 M  $\text{SnCl}_2$  for 10 minutes at 40  $^\circ\text{C}$ . The membranes were then placed in a  $\text{PdCl}_2$  ( $1.4 \times 10^{-3}$  M) solution at 65  $^\circ\text{C}$  for 10 minutes, before being dried in an oven at 85  $^\circ\text{C}$  for 15 minutes. The two-step activation process resulted in the deposition of catalytic Pd nuclei throughout the pores of the membrane, from which Co-B growth is initiated.

The Co-B nanotubes were synthesized via electroless deposition and samples were deposited for periods ranging from 10 to 20 minutes in solutions kept at 65  $^\circ\text{C}$ . The electrolyte comprised of 0.03 M  $\text{CoSO}_4 \cdot 7\text{H}_2\text{O}$ , 0.052 M diammonium citrate, 0.07 M dimethyl amine borane (DMAB) and 0.143 M lactic acid. A pH of 9 was maintained during the deposition by using small additions of concentrated NaOH.

Compositional analysis of the Co-B nanotubes was carried out using X-ray photon spectroscopy (XPS). The electrolessly grown nanotubes were imaged in the field free mode on a Hitachi SU-70 scanning electron microscope (SEM). Images were taken at accelerating voltages up to 30 kV and at working distances as short as 5 mm. Room temperature magnetic measurements of the Co-B nanotubes were measured on a Lakeshore vibrating sample magnetometer (VSM) up to a maximum magnetic field of 1.9 T.

### III. RESULTS AND DISCUSSION

The as-deposited nanostructures, which are formed during the deposition process, consist of nanotubes connected together at both ends by thin films. The external diameter of the nanotubes is controlled by the diameter of the pores in the template, whereas the wall thickness is controlled by the deposition time. Fig. 1 shows SEM images of a typical deposition after the removal of the membrane with concentrated NaOH, which corresponds to a sample deposited for a period of 10 min. The length of the nanotubes ranges from 3 to 6  $\mu\text{m}$ . The nanotube has an external diameter of 450 nm and an inner diameter 360 nm as seen in the inset image. XPS analysis was used to determine the composition of the nanotubes and shows an alloy composition of  $\text{Co}_{70}\text{B}_{30}$ .

The films deposited on the template surfaces were removed by polishing with fine sand paper and membranes were cut into  $5 \times 5 \text{ mm}^2$  for magnetization measurements. Therefore, all the magnetic measurements presented here represent only the magnetic properties of nanotubes. Measurements were carried out at room temperature with a maximum applied field of 1.9 T and magnetization curves are shown in Fig. 2. The specific magnetization varies very little from sample to sample with an average value of  $65.6 \text{ J T}^{-1}\text{kg}^{-1}$ .

We have also investigated the angular dependence of coercivity for the electrolessly deposited array of nanotubes as shown in Fig. 3. The angular dependence of the coercivity on the angles is closely related to the magnetization switching mechanism in the nanotubes.

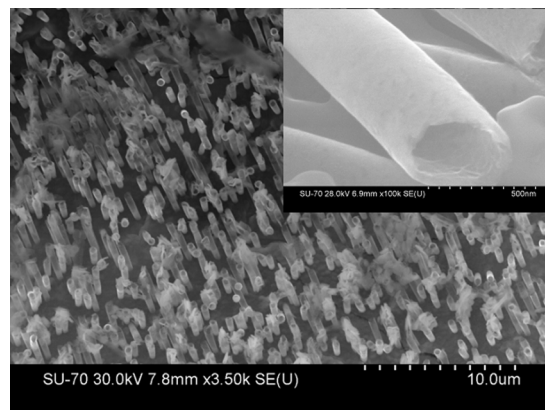


FIG. 1. SEM image of an array of Co-B nanotubes after the removal of the polycarbonate membrane. The inset shows the details of a single nanotube.

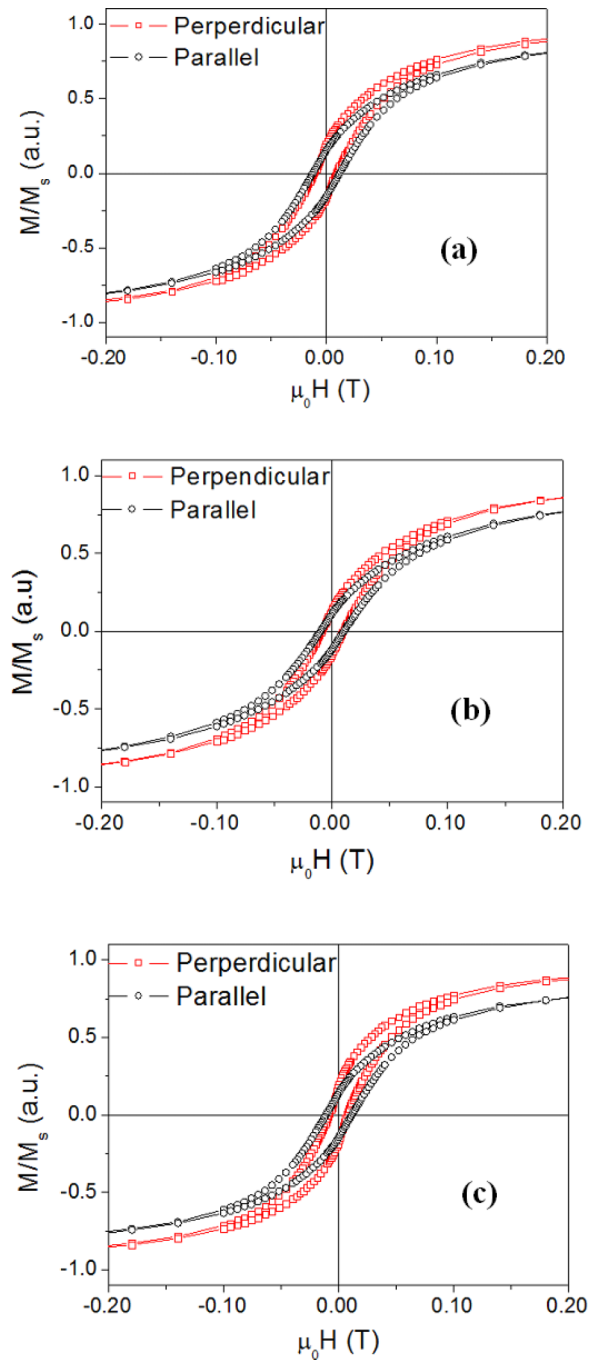


FIG. 2. Room temperature magnetization curves measured perpendicular (open squares) and parallel (open circles) to the long nanotube axis. Nanotubes were deposited for (a) 10 minutes, (b) 15 minutes and (c) 20 minutes.

The mechanism of magnetization reversal in nanotubes can be divided into three categories: coherent rotation, vortex mode and transverse mode. The nanotubes magnetization will tend to reverse via the most energetically favourable mechanism, which in turn determines lowest coercivity of the nanotubes at a given angle. The absolute coercivity values for each mechanism depend on a number of magnetic and structural parameters.

The coherent reversal mechanism is observed in very short nanotubes where the domain wall thickness is of the same order of magnitude as the nanotube length. In our investigation this mechanism can be ruled out as nanotube length is of the order of micronmeter. Therefore, the nanotubes

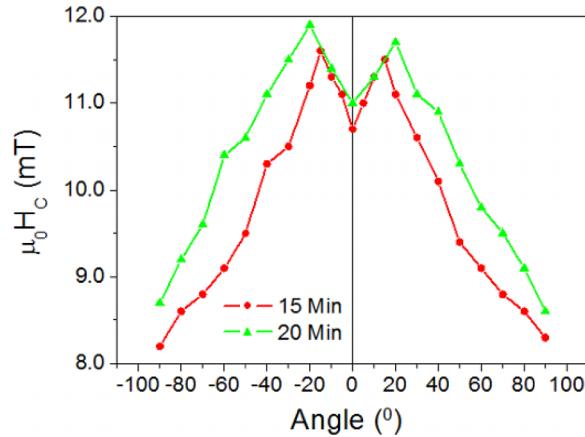


FIG. 3. Angular dependence of coercivity for nanotube arrays deposited for 15 and 20 min. The angle is measured with respect to the long nanotube axis.

presented here can reverse the magnetization via vortex or transverse mechanisms. We observed for Co-B nanotubes that a minimum coercivity perpendicular to the long nanotube axis is obtained as shown in fig. 3. These results contrast to those obtained using a similar preparation method for Ni-B<sup>11</sup> and Ni-Fe-B<sup>12</sup> nanotubes, for which a minimum coercivity is measured parallel to the long nanotube axis. These results indicate that the magnetic reversal mode of Co-B nanotubes differs from those of Ni-B and Ni-Fe-B nanotubes.<sup>11,12</sup>

For vortex mode, also known as a curling reversal mechanism, the magnetic moments of the nanotube reverse via the propagation of a vortex wall along the nanotube axis.<sup>13</sup> The moments are aligned as if they are rotating around the centre of the nanotube axis. Curling mode predicts that the lowest coercivity will be obtained parallel to the long nanotube axis, while the largest coercivity will appear perpendicular to the long nanotube axis.<sup>2</sup>

We observe that the coercivity does not vary monotonically with the angle as shown in Fig. 3. As the angle of applied field with respect to the long nanotube axis decreases, the coercivity of the nanotubes initially increases. However, the maximum coercivity does not occur parallel or perpendicular to the nanotube axis. The maximum coercivity is measured at an angle of approximately 20° for samples prepared for 20 min (fig. 3). This results in an M shaped graph. We can conclude that the maximum coercivity corresponds to the angle at which the magnetic reversal mechanism of the nanotubes switches from a transverse reversal mechanism at large angles to a vortex reversal mechanism at low angles. Stoner and Wohlfarth have shown that coercivity can be expressed in terms of the nucleation field as:

$$|H_C^T(\theta)| = \begin{cases} |H_n^T(\theta)| & \text{for } 0 \leq \theta \leq \pi/4 \\ 2|H_n^T(\pi/4)| - |H_n^T(\theta)| & \text{for } \pi/4 \leq \theta \leq \pi/2 \end{cases} \quad (1)$$

For isolated nanotubes, the angular dependence of the nucleation field is given by Albrecht *et al.* as:<sup>2</sup>

$$H_n^T(\theta) = \frac{2[K(w_T) + K_a]}{\mu_0 M_s^2} \left\{ \frac{1 - f^2(\theta) + f^4(\theta)}{[1 + f^2(\theta)]^2} \right\}^{1/2} M_s \quad (2)$$

Where  $f(\theta) = \tan^{1/3}(\theta)$ ,  $K(w_T) = (1/4)\mu_0 M_s^2 [1 - 3N_Z(w_T)]$  is the shape anisotropy constant,  $K_a$  is the magneto-crystalline constant and  $M_s$  is the saturation magnetization. The combination of coercivity in equation (1) with nucleation field in equation (2) leads to a dependence of coercivity on the angle, which monotonically decreases with increasing angle. If this was the only magnetization reversal mechanism present in the nanotubes, it would be expected that the coercivity should increase as the angle approaches zero and should become maximum at zero. The increase in coercivity with decreasing angle is seen in our data only at angles larger than 20°. On the other hand, the

coercivity due to the nucleation field for vortex mode is a function such as:<sup>2</sup>

$$H_C^V(\theta) \sim H_n^V(\theta) = F(\theta) M_s \quad (3)$$

Where  $F(\theta)$  is the solution of a system of equations combining demagnetizing field, exchange interaction length, nanotube external and internal diameters and the square of the magnetization. Coercivity monotonically increases with increasing angles and shows a minimal value at  $0^\circ$ , which is implicit in equation (3). When the magnetic field is applied parallel to the nanotube axis and the magneto-crystalline anisotropy is negligible, then the equation 3 can be simplified and assumes the following form:<sup>13</sup>

$$H_n^V = \alpha(\beta) \frac{(L_{ex})^2}{R^2} M_s \quad (4)$$

where  $\alpha(\beta)$  is a function of  $\beta$ , which is the ratio given by the internal nanotube radius divided by the external nanotube radius,  $L_{ex}$  is exchange length,  $R$  is the external nanotube diameter and  $M_s$  is the saturation magnetization. The exchange interaction length is given by  $L_{ex} = (2A/(\mu_0 M_s^2))^{1/2}$ , where  $A$  is the exchange stiffness,  $\mu_0$  is permeability of free space. Therefore the nucleation field can be re-written as:

$$H_n^V = \frac{2\alpha(\beta)}{R^2} \left( \frac{A}{\mu_0 M_s} \right) \quad (5)$$

As shown in equation (5), the coercivity associated with the vortex reversal mechanism is directly proportional to the ratio between the exchange stiffness and the magnetization. Taking as an example pure Co with exchange stiffness value of  $3.0 \times 10^{-11} \text{ J m}^{-1}$ <sup>14</sup> and a magnetization of  $\mu_0 M_s = 1.6 \text{ T}$ , one obtains a ratio  $A/(\mu_0 M_s)$  of  $1.87 \times 10^{-11} \text{ J m}^{-1} \text{ T}^{-1}$ , which is larger than that of pure nickel  $1.5 \times 10^{-11} \text{ J m}^{-1} \text{ T}^{-1}$ . Therefore, for the same nanotube geometry, the vortex mode is less energetically favorable for Co than it is for Ni. The addition of B to the alloy reduces both exchange stiffness and saturation magnetization. By comparing Co-B nanotubes to Ni-B nanotubes,<sup>11</sup> we conclude that Co-B has the largest nucleation field for a vortex reversal mechanism, which is only observed at small angles. In addition, in the case of Co-B a crossover between the two switching mechanisms occurs and the overall dependence of coercivity on the angle is no longer a monotonic dependence.

#### IV. CONCLUSION

In conclusion, we have investigated the magnetization reversal switching mechanism of Co-B nanotubes prepared by electroless deposition. Experimental data indicates a change of mechanism, which is dependent on the angle between the applied magnetic field and the long nanotube axis. We interpret this dependence in terms of a crossover from a transverse reversal mechanism to a vortex reversal mechanism at a critical angle, which is about  $20^\circ$  for samples prepared for 20 min. At larger angles the switching mechanism is the transverse mode, whereas at low angle the vortex mode dominates.

#### ACKNOWLEDGMENTS

This work is supported by Science Foundation Ireland (12/IP/1692).

<sup>1</sup> X. Han, S. Shamaila, and R. Sharif, "Ferromagnetic nanowires and nanotubes, electrodeposited nanowires and their applications," in *Electrodeposited Nanowires and their Applications*, edited by Nicoleta Lupu (InTech, 2010), pp. 142–166 Feb.

<sup>2</sup> O. Albrecht, R. Zierold, S. Allende, J. Escrig, C. Patzig, B. Rauschenbach, K. Nielsch, and D. Görnitz, "Experimental evidence for an angular dependent transition of magnetization reversal modes in magnetic nanotubes," *J. Appl. Phys.* **109**(9), 093910 (2011) May.

<sup>3</sup> R. Sharif, S. Shamaila, M. Ma, L.D. Yao, R.C. Yu, X.F. Han, and M. Khaleeq-ur-Rahman, "Magnetic switching of ferromagnetic nanotubes," *Appl. Phys. Lett.* **92**(3), 032505-01–032505-03 (2008) Jan.

- <sup>4</sup> X. Han, S. Shamaïla, R. Sharif, J. Chen, H. Liu, and D. Liu, "Structural and magnetic properties of various ferromagnetic nanotubes," *Adv. Mater.* **21**(45), 1–6 (2009) Dec.
- <sup>5</sup> J. Escrig, M. Daub, P. Landeros, K. Nielsch, and D. Altbir, "Angular dependence of coercivity in magnetic nanotubes," *Nanotech.* **18**(44), 1–5 (2007) Oct.
- <sup>6</sup> F. M. F. Rhen, E. Backen, and J. M. D. Coey, "Thick-film permanent magnets by membrane electrodeposition," *J. Appl. Phys.* **97**(11), 113908-1–113908 (2005) Jun.
- <sup>7</sup> J. F. Rohan, D. P. Casey, B. M. Ahern, F. M. Rhen, S. Roy, D. Fleming, and S. E. Lawrence, "Coaxial metal and magnetic alloy nanotubes in polycarbonate templates by electroless deposition," *Electrochem. Comm.* **10**(9), 1419–1422 (2008) Sept.
- <sup>8</sup> A. Azizi, M. Mohammadi, and S.K. Sadrnezhad, "End-closed NiCoFe-B nanotube arrays by electroless method," *Mater. Lett.* **65**(2), 289–292 (2011) Jan.
- <sup>9</sup> W. Wang, N. Li, X. Li, W. Geng, and S. Qiu, "Synthesis of metallic nanotube arrays in porous anodic aluminum oxide template through electroless deposition," *Mater. Res. Bull.* **41**(8), 1417–1423 (2006) Aug.
- <sup>10</sup> T. Saito, E. Sato, M. Matsuoka, and C. Iwakura, "Electroless deposition of Ni-B, Co-B and Ni-Co-B alloys using dimethylamineborane as a reducing agent.," *J. App. Electrochem.* **28**(5), 559–563 (1998) May.
- <sup>11</sup> D. Richardson and F. M. F. Rhen, "Magnetic properties of electroless deposited Ni-Cu-B nanotube arrays," *IEEE Trans. Magn.* **50**(11), 2303104-1–2303104-4 (2014) Nov.
- <sup>12</sup> D. Richardson, S. Kingston, and F. M. F. Rhen, "Synthesis and characterization of magnetic Ni-Fe-B nanotubes," *IEEE Trans Magn.* (2015) ISSN:0018-9464, May.
- <sup>13</sup> J. Escrig, J. Bachmann, J. Jing, M. Daub, D. Altbir, and K. Nielsch, *Phys. Rev B* **77**, 214421 (2008).
- <sup>14</sup> C.-Y. You, *Appl. Phys. Express* **5**, 103001 (2012).